tic lesions (11). On the other hand, cytosolic DNA has recently been identified as a danger signal that activates inflammasomes containing DNA sensor AIM2 and converting pro-IL-1β to IL-1β (24, 25). LL37 cathelicidin peptide neutralises cytosolic DNA in keratinocytes and blocks inflammasome activation (26). Thus, within keratinocytes, LL37 peptide interferes with DNA-sensing inflammasomes, suggesting an anti-inflammatory function for this cathelicidin peptide.

Therefore it seems that LL37 peptide has contrasting effects in the pathogenesis of psoriasis. On one hand, released LL37 peptide promotes psoriasis *via* interaction with extracellular DNA, but on the other hand, it may suppress psoriasis by interfering cytosolic DNA within the cell. The effect of calcipotriol to increase the intracellular LL37 cathelicidin peptide, along with its potential to decrease the extracellular concentration of LL37, is likely beneficial for the treatment of psoriasis.

The authors declare no conflicts of interest.

REFERENCES

1. Nograles KE, Davidovici B, Krueger JG. New insights in the immunologic basis of psoriasis. Semin Cutan Med Surg 2010; 29: 3–9.
2. Louten J, Boniface K, de Waal Malefyt R. Development and function of TH17 cells in health and disease. J Allergy Clin Immunol 2009; 123: 1004–1011.
3. Koga C, Kabashima K, Shiraishi N, Kobayashi M, Tokura Y. Possible pathogenic role of Th17 cells for atopic dermatitis. J Invest Dermatol 2008; 128: 2625–2630.
4. Dombrowski Y, Schauber J. Cathelicidin LL-37: a defense molecule with a potential role in psoriasis pathogenesis. Exp Dermatol 2012; 21: 327–330.
5. Dürr UH, Sudheendra US, Ramamoorthy A. LL-37, the only human member of the cathelicidin family of antimicrobial peptides. Biochim Biophys Acta 2006; 1758: 1408–1425.
6. Sørensen OE, Follin P, Johnsen AH, Calafat J, Tjabringa GS, Hiemstra PS, Borregaard N. Human cathelicidin, hCAP-18, is processed to the antimicrobial peptide LL-37 by extracellular cleavage with proteinase 3. Blood 2001; 97: 3951–3959.
7. Yamasaki K, Schauber J, Coda A, Lin H, Dorschner RA, Schechter NM, et al. Kallikrein-mediated proteolysis regulates the antimicrobial effects of cathelicidins in skin. FASEB J 2006; 20: 2068–2080.
8. Agerberth B, Charo J, Werr J, Olsson B, Idali F, Lindbom L, et al. The human antimicrobial and chemotactic peptides LL-37 and alpha-defensins are expressed by specific lymphocyte and monocyte populations. Blood 2000; 96: 3086–3093.
9. Niyonsaba F, Iwabuchi K, Someya A, Hirata M, Matsuda H, Ogawa H, Nagaoka I. A cathelicidin family of human antibacterial peptide LL-37 induces mast cell chemotaxis. Immunology 2002; 106: 20–26.
10. De Yang, Chen Q, Schmidt AP, Anderson GM, Wang JM, Wooters J, et al. LL-37, the neutrophil granule- and epithelial cell-derived cathelicidin, utilizes formyl peptide receptor-like 1 (FPRL1) as a receptor to chemoattract human peripheral blood neutrophils, monocytes, and T cells. J Exp Med 2000; 192: 1069–1074.
11. Lande R, Gregorio J, Facchinetti V, Chatterjee B, Wang YH, Homey B, et al. Plasmacytoid dendritic cells sense self-DNA coupled with antimicrobial peptide. Nature 2007; 449: 564–569.
12. De Haes P, Garmyn M, Degreef H, Vantieghem K, Bouillon R, Segaert S. 1,25-Dihydroxyvitamin D3 inhibits ultraviolet B-induced apoptosis, Jun kinase activation, and interleukin-6 production in primary human keratinocytes. J Cell Biochem 2003; 89: 663–673.
13. Koizumi H, Kaplan A, Shimizu T, Ohkawara A. 1,25-Dihydroxyvitamin D3 and a new analogue, 22-oxacalcitriol, modulate proliferation and interleukin-8 secretion of normal human keratinocytes. J Dermatol Sci 1997; 15: 207–213.
14. Fukuoka M, Ogino Y, Sato H, Ohta T, Komoriya K, Nishioka K, Katayama I. RANTES expression in psoriatic skin, and regulation of RANTES and IL-8 production in cultured epidermal keratinocytes by active vitamin D3 (tacalcitol). Br J Dermatol 1998; 138: 63–70.
15. Ghoreishi M, Bach P, Obst J, Komba M, Fleet JC, Dutz JP. Expansion of antigen-specific regulatory T cells with the topical vitamin D analog calcipotriol. J Immunol 2009; 182: 6071–6078.
16. van der Aar AM, Sibiryak DS, Bakdash G, van Capel TM, van der Kleij HP, Opstelten DJ, et al. Vitamin D3 targets epidermal and dermal dendritic cells for induction of distinct regulatory T cells. J Allergy Clin Immunol 2011; 127: 1532–1540.
17. Kobayashi M, Shimauchi T, Hino R, Tokura Y. Roxithromycin downmodulates Th2 chemokine production by keratinocytes and chemokine receptor expression on Th2 cells: its dual inhibitory effects on the ligands and the receptors. Cell Immunol 2004; 228: 27–33.
18. Mori T, Kabashima K, Yoshiki R, Sugita K, Shiraishi N, Onoue A, et al. Cutaneous hypersensitivities to hapten are controlled by IFN-γ-upregulated keratinocyte Th1 chemokines and IFN-γ-downregulated Langerhans cell Th2 chemokines. J Invest Dermatol 2008; 128: 1719–1727.
19. Kang S, Yi S, Griffiths CE, Fancher L, Hamilton TA, Choi JH. Calcipotriene-induced improvement in psoriasis is associated with reduced interleukin-8 and increased interleukin-10 levels within lesions. Br J Dermatol 1998; 138: 77–83.
20. Kim BJ, Rho YK, Lee HI, Jeong MS, Li K, Seo SJ, et al. The effect of calcipotriol on the expression of human beta defensin-2 and LL-37 in cultured human keratinocytes. Clin Dev Immunol 2009; 2009: 645898.
21. Peric M, Koglin S, Kim SM, Morizane S, Besch R, Prinz JC, et al. IL-17A enhances vitamin D3-induced expression of cathelicidin antimicrobial peptide in human keratinocytes. J Immunol 2008; 181: 8504–8512.
22. Heilborn JD, Weber G, Grönberg A, Dieterich C, Ståhle M. Topical treatment with the vitamin D analogue calcipotriol enhances the upregulation of the antimicrobial protein hCAP18/LL-37 during wounding in human skin in vivo. Exp Dermatol 2010; 19: 332–338.
23. Peric M, Koglin S, Dombrowski Y, Eradac E, Büxhau A, Steinmeyer A, et al. Vitamin D analogs differentially control antimicrobial peptide/"alarmin" expression in psoriasis. PLoS One 2009; 4:e6340.
24. Fernandes-Alnemri T, Yu JW, Datta P, Wu J, Alnemri ES. AIM2 activates the inflammasome and cell death in response to cytoplasmic DNA. Nature 2009; 458: 509–513.
25. Hornung V, Ablasser A, Charrel-Dennis M, Bauernfeind F, Horvath G, Caffrey DR, et al. AIM2 recognizes cytosolic dsDNA and forms a caspase-1-activating inflammasome with ASC. Nature 2009; 458: 514–518.
26. Dombrowski Y, Peric M, Koglin S, Kammerbauer C, Göß C, Anz D, et al. Cytosolic DNA Triggers Inflammasome Activation in Keratinocytes in Psoriatic Lesions. Sci Transl Med 2011; 3: 82ra38.

may also be anti-inflammatory by reducing nuclear factor kappa B gene expression.[7] Similarly, in addition to their inflammatory role, Langerhans cells are thought to have immunoregulatory functions.[8] Indeed, we see that langerin$^+$ cells are largely reduced in lesional than in nonlesional AD skin at baseline, and significantly increase on clinical reversal after 12 weeks of CsA treatment (Fig 1, *E*, and Table E3).

In addition to the RDGP, other possible mechanisms for disease recurrence in the same areas need to be considered, including (1) regional differences (increased humidity/friction, transepidermal water loss, pH, and lipids) that allow increased antigen penetration, (2) epigenetic modifications, and (3) microbiome differences.[9]

In summary, we have demonstrated that although the CsA RDGP is much smaller than the NB-UVB RDGP, important structural defects and residual inflammation remain and the overall size of the RDGP does not predict relapse kinetics. Given that NB-UVB and CsA have different courses of disease maintenance on discontinuing therapy, some elements in the RDGP of each treatment might explain relevant treatment- and disease-specific mechanisms.

Mariya Rozenblit, BA[a,b,c]
Mayte Suarez-Farinas, PhD[a,c]
Avner Shemer, MD[d]
Saakshi Khattri, MD[a]
Patricia Gilleaudeau, NP[a]
Mary Sullivan-Whalen, NP[a]
Xiuzhong Zheng, MSc[a]
Hui Xu, MSc[a]
Irma Cardinale, MSc[a]
James G. Krueger, MD, PhD[a,c]
Emma Guttman-Yassky, MD, PhD[a,b]

From [a]the Laboratory for Investigative Dermatology, The Rockefeller University, [b]the Department of Dermatology, Icahn School of Medicine at Mount Sinai, and [c]the Center for Clinical and Translational Science, The Rockefeller University, New York, NY; and [d]the Department of Dermatology, Tel-Hashomer, Tel Aviv, Israel. E-mail: eguttman@rockefeller.edu.

M.R., M.S.-F., and J.G.K. were supported by the National Center for Research Resources (grant no. 5UL1RR024143-02), a component of the National Institutes of Health (NIH), and the NIH Roadmap for Medical Research. E.G.-Y. was supported by the Dermatology Foundation Physician Scientist Career Development Award and by a Clinical and Translational Science Award grant from the Rockefeller University.

Disclosure of potential conflict of interest: J. G. Krueger has received consultancy fees from Centocor, Lilly, and Pfizer and has received research support from Amgen, Centocor, Lilly, Merck, and Pfizer. E. Guttman-Yassky reports grants from Janssen, Merck, Bristol Meyers Squib, and Regeneron; grants and personal fees from Leo-Pharma, Dermira, and Celgene; and personal fees from Genentech, Stiefel/GSK, Pfizer, Medimmune, and Anaptysbio outside the submitted work. The rest of the authors declare that they have no relevant conflicts of interest.

REFERENCES

1. Khattri S, Shemer A, Rozenblit M, Dhingra N, Czarnowicki T, Finney R, et al. Cyclosporine A in atopic dermatitis modulates activated inflammatory pathways and reverses epidermal pathology. J Allergy Clin Immunol 2014;133:1626-34.
2. Suarez-Farinas M, Gittler J, Shemer A, Cardinale I, Krueger JG, Guttman-Yassky E. Residual genomic signature of atopic dermatitis despite clinical resolution with narrow-band UVB. J Allergy Clin Immunol 2012;131:577-9.
3. Leung DY. New insights into atopic dermatitis: a role of skin barrier and immune dysregulation. Allergol Int 2013;62:151-61.
4. Bandow GD, Koo JY. Narrow-band ultraviolet B radiation: a review of the current literature. Int J Dermatol 2004;43:555-61.
5. Granlund H, Erkko P, Sinisalo M, Reitamo S. Cyclosporin in atopic dermatitis: time to relapse and effect of intermittent therapy. Br J Dermatol 1995;132:106-12.
6. Su J, Chen T, Ji XY, Liu C, Yadav PK, Wu R, et al. IL-25 downregulates Th1/Th17 immune response in an IL-10 dependent manner in inflammatory bowel disease. Inflamm Bowel Dis 2013;19:720-8.
7. Ali S, Mohs A, Thomas M, Klare J, Ross R, Schmitz ML, et al. The dual function cytokine IL-33 interacts with the transcription factor NF-kB to dampen NF-kB stimulated gene transcription. J Immunol 2011;187:1609-16.
8. Stoitzner P. The Langerhans cell controversy: are they immunostimulatory or immunoregulatory cells of the skin immune system? Immunol Cell Biol 2010;88:348-50.
9. Flohr C, Mann J. New insights into the epidemiology of childhood atopic dermatitis. Allergy 2014;69:3-16.

Available online July 2, 2014.
http://dx.doi.org/10.1016/j.jaci.2014.05.024

Proteome analysis of stratum corneum from atopic dermatitis patients by hybrid quadrupole-orbitrap mass spectrometer

To the Editor:

The significance of stratum corneum (SC) barrier has been strengthened especially since 2006, when *filaggrin* (*FLG*) mutations and very low expression of profilaggrin/filaggrin monomer were found in patients with atopic dermatitis (AD) as well as ichthyosis vulgaris (IV).[1] Many other SC constituents and proteases are also known to be involved in the barrier, as new susceptibility loci for AD were found by genomewide association study[2] and proteome analysis.[3] Although the SC barrier condition is crucial for the assessment of AD, comprehensive evaluation of its abnormalities in individuals remains to be addressed. It is also notable that AD can be divided into serum IgE-high extrinsic AD (EAD) with impaired barrier and serum IgE-normal intrinsic AD (IAD) with relatively preserved barrier.[4] Here, we sought to identify and quantify wide-ranging proteins by proteome analysis of SC samples obtained by using a noninvasive tape stripping technique.

This study was approved by the Ethical Committee of Hamamatsu University School of Medicine. *EAD* was defined as IgE levels of less than 400 kU/L or 200 < IgE ≤ 400 plus class 2 or more of IgE specific to *Dermatophagoides pteronyssinus* and *Dermatophagoides farinae*, and *IAD* was defined as serum IgE levels of 200 kU/L or less or 200 < IgE ≤ 400 plus class 0 or 1 of the specific IgE.[5] Enrolled in this study were 8 patients with EAD (mean age, 28.1 ± 9.1 years; 5 men, 3 women; mean serum IgE level, 4260.6 ± 5278.9 kU/L), 4 patients with IAD (mean age, 47.8 ± 6.1 years; 1 man, 3 women; mean serum IgE level, 153.8 ± 64.2 kU/L), 3 patients with IV (mean age, 59.3 ± 22.1 years; 3 men), and 3 normal healthy subjects (mean age, 28.3 ± 3.2 years; 3 men). After obtaining informed consent, we collected SC by using a stripping technique with a cellophane tape (Nichiban Co, Tokyo, Japan) from the flexor surface of the forearm of the subjects. The SC-harvested tape was dipped in 10 mL of toluene. After removal of the insoluble tape backing, the sample was centrifuged and the precipitate was washed with toluene 6 times to remove residual adhesives. SC proteins were extracted from the dried sample by solubilization in 50 mM Tris-HCl (pH 6.8) containing 1% SDS and sonication. Acetone-purified extracts were reconstructed with 7 mol/L urea and 50 mM NH_4HCO_3. Ten microgram protein samples were denatured and digested by In-solution tryptic digestion and guanidination kit and purified by C18 spin columns. The samples were solved by 0.1% formic acid solution and analyzed by using Q Exactive hybrid quadrupole-orbitrap mass spectrometer (Thermo Fisher Scientific, Waltham, Mass). By the mass spectrometer and the

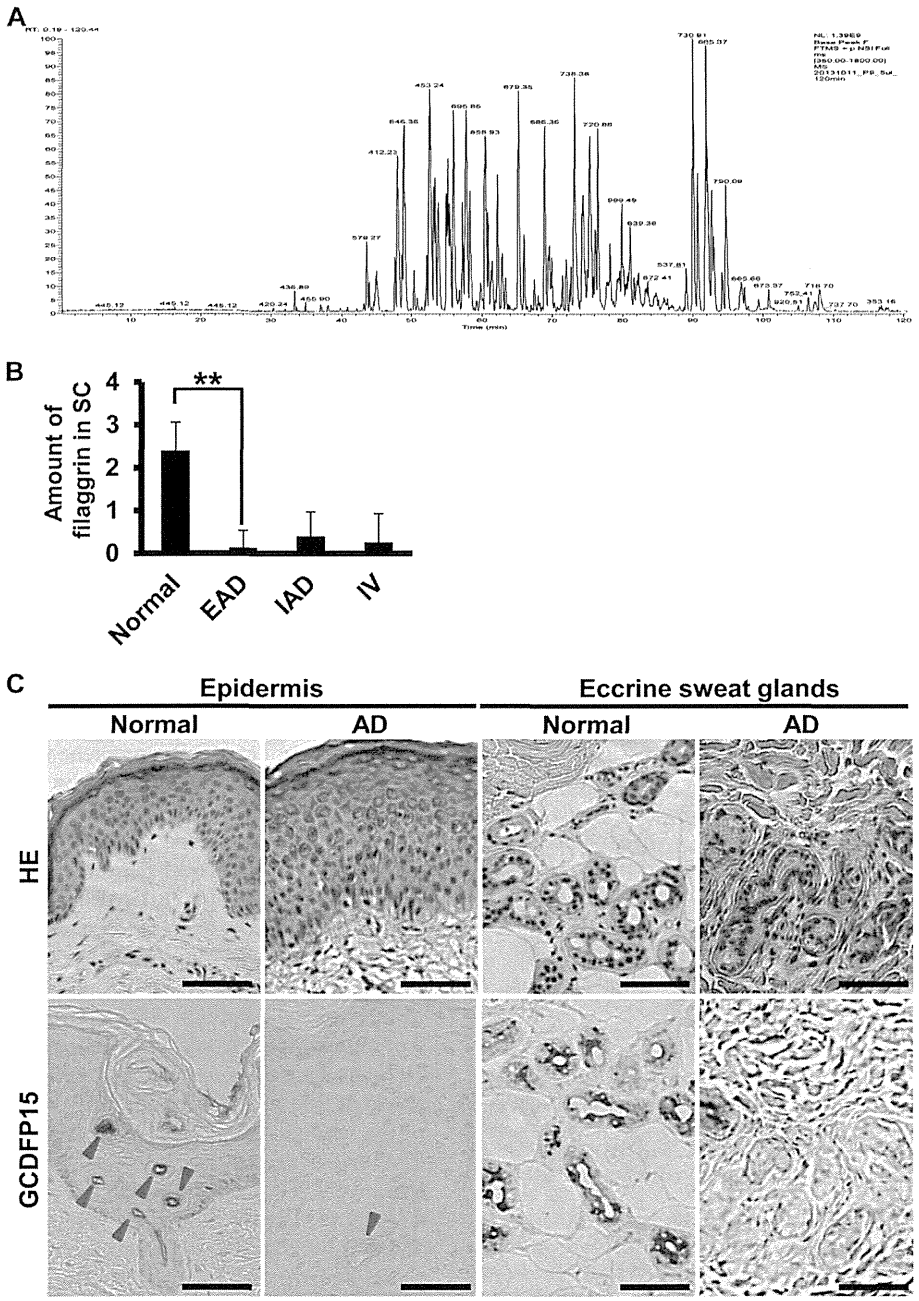

FIG 1. Characterization of patients with AD or IV by liquid chromatography (LC)/MS/MS analysis and immunohistochemistry. **A,** Representative LC/MS/MS analysis of SC. MS spectra were examined in the individual subjects. Note that nonspecific signals, such as polymer and contaminants, were not detected. Substances were detected by using the Mascot search engine (Matrix Science, London, UK; version 2.4) against SwissProt database of human. The amounts of individual proteins were semi-quantified by using the Proteome Discoverer v.1.4 software (Thermo Fisher Scientific). **B,** Comparison of FLG amounts between normal healthy subjects and patients with EAD, IAD, and IV. FLG quantity was decreased in patients with EAD, IAD, and IV than in normal subjects (**$P < .01$). **C,** Representative hematoxylin and eosin staining histopathology of the epidermis and dermal eccrine sweat glands in a normal subject and a patient with EAD. Scale bar is 100 μm *(top).* Representative mmunohistochemical staining for GCDFP15 *(bottom). Red arrowheads,* acrosyringium. Scale bar is 100 μm.

subsequent database analysis (Fig 1, *A*), we identified 421 proteins (see Table E1 in this article's Online Repository at www.jacionline.org). We divided the measurement of each substance by the amount of glyceraldehyde 3-phosphate dehydrogenase. The data were expressed as mean ± SD in each group. The log-transform values were compared between the subject groups by using ANOVA. Furthermore, multiple comparisons of each of the patient groups and healthy controls were conducted by using the Tukey test. See this article's Methods section in the Online Repository at www.jacionline.org.

TABLE I. Categories of representative proteins detected by proteome analysis

Category	SwissProt accession no.	Protein name	Normal (n = 3)	EAD (n = 8)	IAD (n = 4)	IV (n = 3)	*P* value
1. Inflammation-associated substances	P01876	Ig alpha-1 chain C region	0.29	0.68	0.76	0.76	.666
	P01857	Ig gamma-1 chain C region	0.42	4.68*	1.29	1.57	**.006**
	P01859	Ig gamma-2 chain C region	0.34	0.77	0.85	1.40	.589
	P01860	Ig gamma-3 chain C region	0.40	1.68	0.75	1.27	.082
	P01861	Ig gamma-4 chain C region	0.34	1.74	0.85	1.46	.116
	P01834	Ig kappa chain C region	0.37	2.60	1.18	1.13	.122
	P0CG04	Ig lambda-1 chain C regions	0.28	1.39	0.58	0.85	.236
	P02768	Serum albumin	1.44	16.45*	4.70	4.82	**.039**
2. SC barrier constituents	Q15517	Corneodesmosin	1.06	0.88	1.67	1.27	.299
	Q08554	Desmocollin-1	2.17	2.96	3.54	2.41	.783
	Q02413	Desmoglein-1	5.57	7.34	8.90	6.92	.818
	P15924	Desmoplakin	0.60	0.94	0.77	1.54	.111
	P20930	Filaggrin	2.39	0.11*	0.38	0.25	**.015**
	Q5D862	Filaggrin-2	4.59	1.62	3.21	3.63	.333
3. SC barrier–related enzymes	Q13510	Acid ceramidase	0.71	0.43	1.54	1.96	.052
	P05089	Arginase-1	1.21	0.39	1.05	0.53	**.030**
	Q13867	Bleomycin hydrolase	1.13	0.34	1.01	0.56	**.043**
	P07384	Calpain-1 catalytic subunit	0.21	0.20	0.27	0.16	.881
	P31944	Caspase-14	4.29	4.55	5.56	3.61	.873
	P07339	Cathepsin D	0.78	1.43	0.79	1.88	.732
	Q9Y337	Kallikrein-5	0.16	0.40	0.18	0.19	.620
	P49862	Kallikrein-7	0.32	0.55	0.36	0.64	.571
4. Antimicrobial peptides	P31151	Protein S100-A7	0.33	2.37	0.27	0.93	.149
	P05109	Protein S100-A8	0.96	1.88	2.25	2.98	.666
	P06702	Protein S100-A9	1.10	4.48	1.86	4.58	.316
	P81605	Dermcidin	14.63	4.21	3.37	16.10	.229
5. Sweat-associated substances	P12273	Prolactin-inducible protein (GCDFP15)	16.37	3.65†	12.20	32.91	**.023**

P values were calculated by using ANOVA.
Boldface indicates $P < .05$ by ANOVA test.
*$P < .05$ in normal controls vs patients with EAD with Tukey test.
†$P < .05$ in patients with EAD vs IV with Tukey test.

We categorized the representative substances into 5 groups (Table I). In the samples from patients with AD, considerable amounts of inflammation-associated plasma substances (category 1), such as albumin and Ig gamma-1 chain C region fragments, were included. The doses of these substances were higher in patients with EAD than in patients with IAD. Because the intensities of AD and pruritus were comparable between patients with EAD and IAD (SCORing Atopic Dermatitis, 53.2 ± 14.9 vs 46.3 ± 18.5; visual analog scale of pruritus, 64.8 ± 25.2 vs 69.3 ± 39.1), elevation in the levels of inflammatory substances may be a characteristic of EAD. Even the patients with IV, possessing S1701X, S2554X, or S2889X hetrozygous *FLG* mutation, had higher amounts of inflammatory substances than did healthy controls, suggesting that the barrier perturbation may induce subclinical inflammation.

When we focused on category 2 (SC barrier constituents, Table I), FLG was significantly reduced in patients with EAD and also tended to be low in patients with IAD and IV than in normal healthy controls (Fig 1, *B*). Notably, even in patients with IAD, which is considered to have no severely perturbed barrier function,[6] the amount of FLG was low. Although not statistically significant, FLG-2 was decreased in patients with EAD. Desmosome constituents, including corneodesmosin, desmocollin-1, desmoglein-1, and desmoplakin, were not changed among the 4 groups.

In category 3 (SC barrier–related enzymes), acid ceramidase was increased in patients with IAD and IV, suggesting its possible contribution to ceramide deficiency. Arginase-1, bleomycin hydrolase, calpain-1, caspase-14, and cathepsin D are enzymes to process FLG to natural moisturizing factors. Arginase-1 and bleomycin hydrolase were decreased in patients with EAD, as reported previously.[3] Patients with EAD had increased levels of kallikrein 5 and kallikrein 7, which are involved in corneodesmosome cleavage, protease-activated receptor-2 signal induction, and profilaggrin processing,[7] consistent with previous observations.[8]

Among antimicrobial peptides (category 4), there was a tendency that dermcidin, but not the other proteins, was reduced in patients with EAD and IAD. This suggests that the impaired defense against microbes may be attributable to the reduced production of dermcidin.

Category 5 is represented by prolactin-inducible protein (also known as gross cystic disease fluid protein 15 [GCDFP15]), whose amount was significantly reduced in patients with EAD. Because GCDFP15 is produced by sweat glands,[9] our data presumably reflect the decreased sweating in patients with AD. The reduced production of GCDFP15 was confirmed by immunohistochemical staining of eccrine sweat glands, which showed the positive staining of the epidermal acrosyringium (Fig 1, *C*, left) and the secretary potion of dermal eccrine glands (Fig 1, *C*, right) in the skin of normal healthy persons but not in the skin of patients with AD.

The present proteome study allows us to quantify wide-ranging proteins in SC, and AD is a representative target for this analysis. The clinical accuracy and applicability of this analysis were proven by the reduction in FLG in patients with EAD. Information obtained from this comprehensive study is useful not only for the evaluation of the patient's SC condition but also for the detection of critical proteins involved in the pathogenesis of AD.

Jun-Ichi Sakabe, PhD[a]
Koji Kamiya, MD, PhD[a]
Hayato Yamaguchi, MD[a]
Shigeki Ikeya, MD[a]
Takahiro Suzuki, MD[a]
Masahiro Aoshima, MD[a]
Kazuki Tatsuno, MD[a]
Toshiharu Fujiyama, MD[a]
Masako Suzuki[b]
Tsuyoshi Yatagai, MD[a]
Taisuke Ito, MD, PhD[a]
Toshiyuki Ojima, MD, PhD[c]
Yoshiki Tokura, MD, PhD[a]

From [a]the Department of Dermatology, [b]the Equipment Center, and [c]the Department of Community Health and Preventive Medicine, Hamamatsu University School of Medicine, Hamamatsu, Japan. E-mail: jsakabe@hama-med.ac.jp.

This work was supported by a Grant-in-Aid for Young Scientists (B) (grant no. 26860877 to J.-I.S.) and a Grant-in-Aid for Exploratory Research (grant no. 26670524 to Y.T.) from the Ministry of Education, Culture, Sports, Science and Technology.

Disclosure of potential conflict of interest: J.-I. Sakabe has received research support from the Ministry of Education, Culture, Sports, Science and Technology (MEXT; 26860877). Y. Tokura has received research support from Ministry of Education, Culture, Sports, Science, and Technology (MEXT; 26670524); has received consultancy fees from Torii Pharm; has provided expert testimony for Galderma; has received research support from Jansen; and has received lecture fees from GSK, Novartis, Tanabe Mitsubishi, and Daiichi-Sankyo. The rest of the authors declare that they have no relevant conflicts of interest.

REFERENCES

1. Sandilands A, Terron-Kwiatkowski A, Hull PR, O'Regan GM, Clayton TH, Watson RM, et al. Comprehensive analysis of the gene encoding filaggrin uncovers prevalent and rare mutations in ichthyosis vulgaris and atopic eczema. Nat Genet 2007;39:650-4.
2. Hirota T, Takahashi A, Kubo M, Tsunoda T, Tomita K, Sakashita M, et al. Genome-wide association study identifies eight new susceptibility loci for atopic dermatitis in the Japanese population. Nat Genet 2012;44:1222-6.
3. Broccardo CJ, Mahaffey S, Schwarz J, Wruck L, David G, Schlievert PM, et al. Comparative proteomic profiling of patients with atopic dermatitis based on history of eczema herpeticum infection and *Staphylococcus aureus* colonization. J Allergy Clin Immunol 2011;127:186-93, 193.e1-11.
4. Tokura Y. Extrinsic and intrinsic types of atopic dermatitis. J Dermatol Sci 2010;58:1-7.
5. Yamaguchi H, Kabashima-Kubo R, Bito T, Sakabe J, Shimauchi T, Ito T, et al. High frequencies of positive nickel/cobalt patch tests and high sweat nickel concentration in patients with intrinsic atopic dermatitis. J Dermatol Sci 2013;72:240-5.
6. Mori T, Ishida K, Mukumoto S, Yamada Y, Imokawa G, Kabashima K, et al. Comparison of skin barrier function and sensory nerve electric current perception threshold between IgE-high extrinsic and IgE-normal intrinsic types of atopic dermatitis. Br J Dermatol 2010;162:83-90.
7. Sakabe J, Yamamoto M, Hirakawa S, Motoyama A, Ohta I, Tatsuno K, et al. Kallikrein-related peptidase 5 functions in proteolytic processing of profilaggrin in cultured human keratinocytes. J Biol Chem 2013;288:17179-89.
8. Komatsu N, Saijoh K, Kuk C, Liu AC, Khan S, Shirasaki F, et al. Human tissue kallikrein expression in the stratum corneum and serum of atopic dermatitis patients. Exp Dermatol 2007;16:513-9.
9. Myal Y, Robinson DB, Iwasiow B, Tsuyuki D, Wong P, Shiu RP. The prolactin-inducible protein (PIP/GCDFP-15) gene: cloning, structure and regulation. Mol Cell Endocrinol 1991;80:165-75.

http://dx.doi.org/10.1016/j.jaci.2014.07.054

Trends in hospitalizations for food-induced anaphylaxis in US children, 2000-2009

To the Editor:

By most estimates, the US prevalence of food allergies has been increasing. Earlier studies also support a corresponding escalation in health care utilization for food-induced anaphylaxis (FIA), including increased numbers of emergency department (ED) visits and hospitalizations.[1-3] In contrast, a recently published article by our group reported that FIA-related ED visits did not differ statistically for children younger than 18 years between 2001 and 2009.[4] To more fully understand these trends in anaphylaxis care, we used a nationally representative pediatric database to describe the frequency and characteristics of FIA hospitalizations in children over the same time period (2000-2009).

Data were obtained from the Healthcare Cost and Utilization Project Kids' Inpatient Database, the only all-payer pediatric inpatient care database in the United States. The Healthcare Cost and Utilization Project Kids' Inpatient Database consists of a stratified random sample of 12,039,432 inpatient discharges from 27 to 44 states during the 4 periods of our study: 2000, 2003, 2006, and 2009. See this article's Online Repository at www.jacionline.org for a description of data collection and estimation procedures.[5] Our analysis was exempted from human subjects review by our institutional review board.

Patients younger than 18 years were included if 1 of the first 3 diagnosis categories included a relevant diagnosis code for FIA[6]: dermatitis due to food (693.10); anaphylactic shock due to adverse food reaction (995.60-995.69); adverse food reaction, not elsewhere classified (995.70); or other anaphylactic shock (995.00). Sensitivity analyses were performed with (1) more inclusive codes (693.10, 995.00, 995.3 [allergy, unspecified, not elsewhere classified], 995.60-995.69, 995.70); (2) more exclusive codes (693.10, 995.60-995.69, 995.70); and (3) limiting food allergy codes to the first diagnostic category only.

FIA visit rates were calculated and analyzed by age, sex, race (white, black, Asian/Pacific islander, other), Hispanic ethnicity, US region (Northeast, Midwest, South, West), and hospital location/teaching status (rural, urban/teaching, urban/nonteaching). Total costs were estimated by applying the Healthcare Cost and Utilization Project Cost-to-Charge Ratio Files.[5] All charges (amount hospital billed for services) and costs

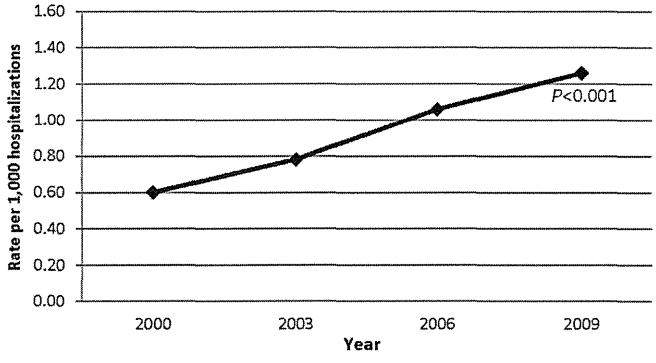

FIG 1. Food-induced anaphylaxis hospitalizations (per 1000 total hospitalizations), by year.

METHODS

Sample collection and storage

The study was approved by the Ethical Committee of Hamamatsu University School of Medicine and performed at the University Hospital of Hamamatsu University School of Medicine. Written informed consent was obtained from all subjects. Human SC samples were obtained from the forearms and upper arms of 3 normal volunteers (3 men; age, 28.3 ± 3.2 years), 8 patients with EAD (5 men and 3 women; age, 28.1 ± 9.1 years), 4 patients with IAD (1 man and 3 women; age, 47.8 ± 6.1 years), and 3 patients with IV (3 men; age, 59.3 ± 22.1 years). Tape stripping was performed at least 24 hours after the last topical application. On sampling, we avoided the skin with severe eczema, moderate to strong lichenification, excoriation, crust, and secondary infection and the skin in joint areas. The SC was obtained by stripping using the Nichiban cellophane tape (organic solvent-stable tape with organic solvent-soluble adhesive; Nichiban, Tokyo, Japan). The tape was applied to the flexor surface of the subjects' forearm and the upper arm. SC samples were obtained from 12 different places using 10 cm length of Nichiban tape. The SC samples on the tape were immediately stored at −20°C until treatment with toluene. When the tape was dipped in 10 mL of toluene, all adhesives were dissolved and any attached SC was suspended. After the insoluble tape backing was removed, the sample was centrifuged at 3000 rpm for 15 minutes. The precipitate was washed with 5 mL of toluene 6 times to remove any residual adhesive. After the toluene treatment, the purified samples were air dried, weighed, and kept at −20°C.

Protein extraction and purification

Dried SC samples were dissolved by 1% SDS lysis buffer (50 mM Tris HCl, pH 6.8, and 1% SDS) in 1.5 mL protein LoBind tube (Eppendorf, Hamburg, Germany). The samples were then homogenated and sonicated for 20 minutes (interval, 30 seconds; sonication, 30 seconds). The suspension was centrifuged at 13,000 rpm for 15 minutes at 4°C. The supernatant was collected and put into a fresh 1.5-mL protein LoBind tube, and 100% acetone was added at 10 times of the sample volume. It was incubated at −80°C overnight and centrifuged at 15,000 rpm for 30 minutes at 4°C. The supernatant was discarded and the pellet was completely dried by using an evaporator for 15 to 30 minutes at room temperature. Dehydrated pellet was dissolved in 10 μL of 7 mol/L urea for 30 minutes at 60°C. Furthermore, 90 μL of 50 mM ammonium bicarbonate was added to the sample solution. Protein concentration was measured by using the Lowry method with DC Protein assay kit (Bio-Rad, Hercules, Calif). All reagents used were Liquid Chromatography - Mass Spectrometry grade.

Protein digestion

Ten microgram proteins were denatured with No-Weight DTT (Thermo Fisher Scientific) for 5 minutes at 95°C and alkylated by iodoacetamide (Thermo Fisher Scientific) for 20 minutes in the dark at room temperature. After 20 minutes, activated trypsin protease, MS grade (Thermo Fisher Scientific), was added to the sample and incubated overnight at 37°C. Trypsin protease reaction was stopped by trifluoroacetic acid (Thermo Fisher Scientific). Peptides were purified with Pierce C18 Spin Columns (Thermo Fisher Scientific), according to the manufacturer's instructions. Purified peptides were dried by using an evaporator at room temperature. Finally, peptides were dissolved in 0.1% formic acid (Thermo Fisher Scientific). All reagents used were LC/MS grade.

Liquid chromatography/MS/MS analysis

Peptides suspension dissolved in 0.1% formic acid was analyzed by using Q Exactive (Thermo Fisher Scientific). Liquid chromatography was carried out using a Thermo Easy-nLC 1000 HPLC equipped using a C-18 column (3 μm particle size, 150 × 0.075 mm internal diameter) (Nikkyo Technos, Co, Ltd, Tokyo, Japan). Eluted peptides were analyzed on Nanospray Flex Ion Source. Buffer A for the pump consisted of 0.1% formic acid in LC/MS-grade water; buffer B for the pump consisted of 0.1% formic acid in LC/MS-grade acetonitrile. Gradient conditions for pump B were as follows: 0% to 35% B from 0 to 120 minutes. A total of 5 μL of the prepared peptides was injected onto the enrichment column for concentration/purification. Flow rates were 300 nL/min. Some parameters in Orbitrap were as follows: spray voltage, 2.0 kV; capillary temperature, 250°C; *m/z* (mass to charge ratio) range (ms), 350 to 1800. AGC ion injection targets for each FTMS scan were 70,000 (60 ms max injection time). AGC ion injection targets for each MS^2 scan were 17,500 (50 ms max ion injection time). Full MS/dd-MS^2 (Top10) was used in this analysis.

Database searching

The raw data was processed using Proteome Discoverer (version 1.4.0.288, Thermo Fischer Scientific). MS/MS spectra were searched with Mascot (version 2.4, Matrix Science, London, United Kingdom) engine against the SwissProt *Homo sapiens* protein sequence database. Peptides were generated from a tryptic digestion with up to 2 missed cleavages, dynamic modifications of methionine oxidation, and a static modification of cysteine carbamidomethylation. Precursor mass tolerance was 10 ppm, and product ions were searched at 0.02-Da tolerances. Peptide spectral matches were validated using percolator based on q values at a 1% false discovery rate.[E1]

Protein selection

For each of the 18 tissue specimen data files (3 normal healthy, 8 EAD, 4 IAD, and 3 IV), Proteome Discover was used to export the list of identified proteins to Excel. For quantification purposes, we utilized the node "The Precursor Ions Area Detector" of Proteome Discoverer, which calculates the area under the curve of each precursor ion using integration. For greater accuracy, it uses an average of the 3 most abundant peptides per protein rather than all peptides per protein to calculate the protein area. The number of peptide spectral matches for each protein in each sample was also used for quantification (spectral counting). We exported a table from Proteome Discoverer that contained SwissProt accession numbers, protein names, the number of peptide spectrum matches, and the protein area for each protein from each sample file. Both the number of spectral counts and the protein area estimates for each protein in each sample were used for further statistical validation. Unmodified/modified and shared (homologous) peptides were also present in the output list from Proteome Discoverer. Dynamic exclusion was set to 10 s.

Statistical analysis

Protein production levels were normalized by glyceraldehyde 3-phosphate dehydrogenase, and these log-transform values were compared between 4 types of groups (healthy, EAD, IAD, and IV) by using ANOVA. Furthermore, multiple comparisons of each of the EAD, IAD, IV groups and healthy controls were conducted by using the Tukey test.

REFERENCE

E1. Brosch M, Yu L, Hubbard T, Choudhary J. Accurate and sensitive peptide identification with mascot percolator. J Proteome Res 2009;8:3176-81.

TABLE E1. Complete list of proteins identified by using liquid chromatography/MS/MS analysis

SwissProt accession no.	Protein name
P62258	14-3-3 protein epsilon
P31947	14-3-3 protein sigma
P63104	14-3-3 protein zeta/delta
P11021	78-kDa glucose-regulated protein
Q13510	Acid ceramidase
P60709	Actin, cytoplasmic 1
O75608	Acyl-protein thioesterase 1
P05141	ADP/ATP translocase 2
P61204	ADP-ribosylation factor 3
Q9UKK9	ADP-sugar pyrophosphatase
Q8TDN7	Alkaline ceramidase 1
P02763	Alpha-1-acid glycoprotein 1
P19652	Alpha-1-acid glycoprotein 2
P01011	Alpha-1-antichymotrypsin
P01009	Alpha-1-antitrypsin
P04217	Alpha-1B-glycoprotein
P01023	Alpha-2-macroglobulin
A8K2U0	Alpha-2-macroglobulin-like protein 1
P12814	Alpha-actinin-1
P49419	Alpha-aminoadipic semialdehyde dehydrogenase
P04745	Alpha-amylase 1
P06733	Alpha-enolase
P06280	Alpha-galactosidase A
P00709	Alpha-lactalbumin
Q16706	Alpha-mannosidase 2
P17050	Alpha-*N*-acetylgalactosaminidase
P04083	Annexin A1
P07355	Annexin A2
P09525	Annexin A4
P08758	Annexin A5
P02647	Apolipoprotein A-I
P02652	Apolipoprotein A-II
P04114	Apolipoprotein B-100
P05090	Apolipoprotein D
O75342	Arachidonate 12-lipoxygenase, 12R-type
O43150	Arf-GAP with SH3 domain, ANK repeat, and PH domain–containing protein 2
P05089	Arginase-1
P54793	Arylsulfatase F
P61769	Beta-2-microglobulin
Q562R1	Beta-actin-like protein 2
P05814	Beta-casein
P16278	Beta-galactosidase
P08236	Beta-glucuronidase
P07686	Beta-hexosaminidase subunit beta
Q13867	Bleomycin hydrolase
Q9NP55	BPI fold-containing family A member 1
Q8TDL5	BPI fold-containing family B member 1
Q9NXV2	BTB/POZ domain–containing protein KCTD5
P12830	Cadherin-1
Q13557	Calcium/calmodulin-dependent protein kinase type II subunit delta
P62158	Calmodulin
P27482	Calmodulin-like protein 3
Q9NZT1	Calmodulin-like protein 5
Q96L46	Calpain small subunit 2
P07384	Calpain-1 catalytic subunit
P00915	Carbonic anhydrase 1
P00918	Carbonic anhydrase 2
P23280	Carbonic anhydrase 6
Q9UI42	Carboxypeptidase A4
P16870	Carboxypeptidase E
P14384	Carboxypeptidase M
P31944	Caspase-14

(Continued)

TABLE E1. *(Continued)*

SwissProt accession no.	Protein name
P04040	Catalase
P49913	Cathelicidin antimicrobial peptide
P07858	Cathepsin B
P07339	Cathepsin D
P08311	Cathepsin G
O60911	Cathepsin L2
P20645	Cation-dependent mannose-6-phosphate receptor
P13987	CD59 glycoprotein
P00450	Ceruloplasmin
P36222	Chitinase-3-like protein 1
Q15782	Chitinase-3-like protein 2
O14493	Claudin-4
P10909	Clusterin
P35606	Coatomer subunit beta
P23528	Cofilin-1
A6NC98	Coiled-coil domain-containing protein 88B
P01024	Complement C3
P0C0L4	Complement C4-A
Q07021	Complement component 1 Q subcomponent-binding protein, mitochondrial
Q15517	Corneodesmosin
Q9BYD5	Cornifelin
P06732	Creatine kinase M-type
P12532	Creatine kinase U-type, mitochondrial
Q9UJ71	C-type lectin domain family 4 member K
P01040	Cystatin-A
P04080	Cystatin-B
Q15828	Cystatin-M
P01036	Cystatin-S
P54108	Cysteine-rich secretory protein 3
Q07065	Cytoskeleton-associated protein 4
Q9UGM3	Deleted in malignant brain tumors 1 protein
Q8NFT8	Delta and Notch-like epidermal growth factor–related receptor
O76062	Delta(14)-sterol reductase
P13716	Delta-aminolevulinic acid dehydratase
P81605	Dermcidin
Q6E0U4	Dermokine
Q08554	Desmocollin-1
Q02487	Desmocollin-2
Q14574	Desmocollin-3
Q02413	Desmoglein-1
P15924	Desmoplakin
P09622	Dihydrolipoyl dehydrogenase, mitochondrial
Q01459	Di-*N*-acetylchitobiase
P53634	Dipeptidyl peptidase 1
Q9UHL4	Dipeptidyl peptidase 2
P27487	Dipeptidyl peptidase 4
P39656	Dolichyl-diphosphooligosaccharide–protein glycosyltransferase 48-kDa subunit
P04843	Dolichyl-diphosphooligosaccharide–protein glycosyltransferase subunit 1
P61803	Dolichyl-diphosphooligosaccharide–protein glycosyltransferase subunit DAD1
P46977	Dolichyl-diphosphooligosaccharide–protein glycosyltransferase subunit STT3A
Q8TEA8	D-tyrosyl-tRNA(Tyr) deacylase 1
P68104	Elongation factor 1-alpha 1
P13639	Elongation factor 2
P61916	Epididymal secretory protein E1
P58107	Epiplakin
P24390	ER lumen protein retaining receptor 1
P56537	Eukaryotic translation initiation factor 6
Q16610	Extracellular matrix protein 1
Q01469	Fatty acid–binding protein, epidermal
Q6ZVX7	F-box only protein 50
P02671	Fibrinogen alpha chain
P02675	Fibrinogen beta chain

(Continued)

TABLE E1. *(Continued)*

SwissProt accession no.	Protein name
P02679	Fibrinogen gamma chain
Q9BYJ0	Fibroblast growth factor–binding protein 2
P02751	Fibronectin
P20930	Filaggrin
Q5D862	Filaggrin-2
P21333	Filamin-A
O75369	Filamin-B
P17931	Galectin-3
Q08380	Galectin-3–binding protein
P47929	Galectin-7
Q92820	Gamma-glutamyl hydrolase
O75223	Gamma-glutamylcyclotransferase
P13284	Gamma-interferon–inducible lysosomal thiol reductase
P17900	Ganglioside GM2 activator
Q96QA5	Gasdermin-A
P06396	Gelsolin
P04062	Glucosylceramidase
Q16769	Glutaminyl-peptide cyclotransferase
P35754	Glutaredoxin-1
P09211	Glutathione S-transferase P
P48637	Glutathione synthetase
P04406	Glyceraldehyde-3-phosphate dehydrogenase
Q7L5L3	Glycerophosphodiester phosphodiesterase domain–containing protein 3
P28799	Granulins
P63244	Guanine nucleotide-binding protein subunit beta-2-like 1
P00739	Haptoglobin-related protein
P08107	Heat shock 70-kDa protein 1A/1B
P11142	Heat shock cognate 71-kDa protein
P04792	Heat shock protein beta-1
P54652	Heat shock–related 70-kDa protein 2
Q9Y5Z4	Heme-binding protein 2
P69905	Hemoglobin subunit alpha
P68871	Hemoglobin subunit beta
P02042	Hemoglobin subunit delta
P02790	Hemopexin
P42357	Histidine ammonia-lyase
P04196	Histidine-rich glycoprotein
Q96KK5	Histone H2A type 1-H
O60814	Histone H2B type 1-K
P62805	Histone H4
P04229	HLA class II histocompatibility antigen, DRB1-1 beta chain
Q86YZ3	Hornerin
Q9BYJ1	Hydroperoxide isomerase ALOXE3
P22304	Iduronate 2-sulfatase
P01876	Ig alpha-1 chain C region
P01877	Ig alpha-2 chain C region
P01857	Ig gamma-1 chain C region
P01859	Ig gamma-2 chain C region
P01860	Ig gamma-3 chain C region
P01861	Ig gamma-4 chain C region
P01825	Ig heavy chain V-II region NEWM
P01772	Ig heavy chain V-III region KOL
P01777	Ig heavy chain V-III region TEI
P01765	Ig heavy chain V-III region TIL
P01834	Ig kappa chain C region
P01619	Ig kappa chain V-III region B6
P01620	Ig kappa chain V-III region SIE
P01625	Ig kappa chain V-IV region Len
P80748	Ig lambda chain V-III region LOI
P01714	Ig lambda chain V-III region SH
P0CG04	Ig lambda-1 chain C regions
P0CG05	Ig lambda-2 chain C regions

(Continued)

TABLE E1. *(Continued)*

SwissProt accession no.	Protein name
P04220	Ig mu heavy chain disease protein
P01591	Immunoglobulin J chain
P12268	Inosine-5′-monophosphate dehydrogenase 2
O14732	Inositol monophosphatase 2
P14735	Insulin-degrading enzyme
Q9NZH8	Interleukin-36 gamma
Q9NZH6	Interleukin-37
Q6ZNF0	Iron/zinc purple acid phosphatase-like protein
P14923	Junction plakoglobin
O43240	Kallikrein-10
Q9UBX7	Kallikrein-11
Q9P0G3	Kallikrein-14
Q9Y337	Kallikrein-5
P49862	Kallikrein-7
O60259	Kallikrein-8
Q9UKQ9	Kallikrein-9
Q15323	Keratin, type I cuticular Ha1
P13645	Keratin, type I cytoskeletal 10
P13646	Keratin, type I cytoskeletal 13
P02533	Keratin, type I cytoskeletal 14
P19012	Keratin, type I cytoskeletal 15
P08779	Keratin, type I cytoskeletal 16
Q04695	Keratin, type I cytoskeletal 17
Q9C075	Keratin, type I cytoskeletal 23
P35527	Keratin, type I cytoskeletal 9
P04264	Keratin, type II cytoskeletal 1
Q7Z794	Keratin, type II cytoskeletal 1b
P35908	Keratin, type II cytoskeletal 2 epidermal
P12035	Keratin, type II cytoskeletal 3
P19013	Keratin, type II cytoskeletal 4
P13647	Keratin, type II cytoskeletal 5
P02538	Keratin, type II cytoskeletal 6A
P48668	Keratin, type II cytoskeletal 6C
P08729	Keratin, type II cytoskeletal 7
Q86Y46	Keratin, type II cytoskeletal 73
O95678	Keratin, type II cytoskeletal 75
Q8N1N4	Keratin, type II cytoskeletal 78
Q6KB66	Keratin, type II cytoskeletal 80
A6NCN2	Keratin-81-like protein KRT121P
Q5T749	Keratinocyte proline-rich protein
P02788	Lactotransferrin
Q659C4	La-related protein 1B
Q9BS40	Latexin
Q9UIQ6	Leucyl-cystinyl aminopeptidase
P30740	Leukocyte elastase inhibitor
P31025	Lipocalin-1
P00338	L-lactate dehydrogenase A chain
Q7Z4W1	L-xylulose reductase
Q9BZG9	Ly-6/neurotoxin-like protein 1
O95274	Ly6/PLAUR domain–containing protein 3
Q6UWN5	Ly6/PLAUR domain–containing protein 5
O95867	Lymphocyte antigen 6 complex locus protein G6c
P10253	Lysosomal alpha-glucosidase
O00754	Lysosomal alpha-mannosidase
P10619	Lysosomal protective protein
P42785	Lysosomal Pro-X carboxypeptidase
Q14108	Lysosome membrane protein 2
P11279	Lysosome-associated membrane glycoprotein 1
P13473	Lysosome-associated membrane glycoprotein 2
P61626	Lysozyme C
P40121	Macrophage-capping protein
P40926	Malate dehydrogenase, mitochondrial

(Continued)